FINITE ELEMENT ANALYSIS OF VIOLIN SHELL MODES

C Gough, School of Physics and Astronomy, University of Birmingham

1 INTRODUCTION

Over the last few years there has been a dramatic increase in the number of acoustic measurements on outstanding Cremonese violins. However, there is still no consensus on the relationship between their acoustical properties and perceived quality.

Of particular note have been the modal analysis measurements of George Bissinger[1,2] at the University of East Carolina, which now includes results from the recent 3D laser-scanning project undertaken in collaboration with two leading American violin makers, Joe Curtin and Sam Zygmuntowicz, and Fan Tao of D'Arradio Strings. This project has produced detailed 3-D information of the vibrations and associated acoustic radiation of the 1715 Titian and 1734 Willemotte Stradivari and 1735 Plowden Guarneri del Gesu violins. In addition, there are now a large number of admittance and acoustic radiation measurements on more than a dozen Stradivari and Guarneri violins and other fine Cremonese and modern instruments – and a few "bad" instruments for comparison.

All such measurements confirm the acoustic importance of the low frequency "signature" modes: the A0 air resonance at ~ 280Hz, the CBR centre bout rotation mode at ~ 350-450 Hz, and the two strongly radiating B1- and B1+, often referred to as "corpus bending" modes, at typical frequencies in the range 370 – 450Hz and 520-580Hz respectively. These modes determine the strength of the first and second partials of all bowed note sounds below the open E-string, and must therefore be important in determining the perceived quality, though the amplitudes of partials at higher frequencies are equally important in assessing quality across the whole playing range.

The primary objective of the present proposal is to develop a FEA model of the violin, with fully adjustable parameters - like plate thicknesses, elastic properties and arching, sound post properties and position, rib thicknesses and heights, bridge geometry and resonances, *f*-hole shape and elastic properties of the central island area, bass bar size, etc – to address violin maker's frequent questions on how such parameters affect the position and strength of the easily measured signature modes and perceived quality of an instrument. A second objective is to achieve a better understanding of the origin and nature of the CBR, B1- and B1+ modes than currently exists.

Our aim is to produce a model that reproduces generic properties of violin dynamics and radiation rather than attempt precise modeling of a specific instrument. We aim to understand how the normal modes of the instrument change in frequency, mode shape, effective mass at the bridge and radiation efficiency, as any one of the above parameters is changed. To elucidate the physics, such parameters can be varied over several orders of magnitude – which is easy to investigate on a computer model but impossible for a real violin.

A number of detailed FEA calculations for the violin have been published, notably the first such studies by Knott[3] and Roberts[4]. In the latter case, the eigen-modes of the instrument were followed at all stages of the making of the violin, from individual plates to assembled instrument with bass bar, *f*-holes and soundpost. These early calculations were based on main-frame computers using powerful, though time-consuming and relatively sophisticated, FEA software. In this study we use the COMSOL FEA 3D shell structure graphical software package running on a desk-top computer, which typically allows one to evaluate the lowest 40 or so eigen frequencies and mode shapes for a typical violin shell shape with f-holes, bass bar, sound post and bridge in a few seconds. The only complication is the need to deal with anisotropic elastic properties, for which the necessary shell software has not yet been written - though it could be programmed to do so by an expert user. We have adopted an alternative approach by creating the plates as composite structures with thin strips parallel to the wood grain, with alternating high and low elastic constants to mimic the rather more finely grained structure of spruce and maple plates.

Because the vibrational states of the fully assembled violin are relatively complicated modes of mixed symmetry, we have chosen to start by treating the violin as a geometrically symmetrical shell structure supporting easily understood symmetric and asymmetric vibrational modes. We then investigate how such modes are mixed on cutting f-holes, inserting the soundpost, etc.

The modes of the assembled instrument involve the strong coupling of the front and back plates by the ribs. By varying the rib coupling strength over many orders of magnitude, we show that the modes of a representative guitar-shaped violin body are of two quite distinct types – *corpus modes,* with identical displacements of the front and back plates, and *plate modes* involving flexural waves on both front and back plates. For any thin shell geometry the corpus and plate modes can be distinguished by their different dependencies on film thickness and rib coupling.

Plots of modal frequencies against rib strength show that most corpus and plate modes are only weakly coupled. We illustrate the very strong perturbation of the plate modes by the soundpost, which acts as rigid connection between the plates at all frequencies of interest.

In the second part of this paper, we illustrate the importance of the soundpost by results from a preliminary study on a simple Savart trapezoidal flat plate violin[5]. FEA predictions indicate the importance of the soundpost position in determining mode shapes in the island area between the *f*-holes and hence the coupling of the plates to the bowed strings via the bridge. This is illustrated by varying the soundpost offset distance from the central axis and its placement towards and away from the upper bout. Although such calculations have currently only been completed for the Savart violin, we would expect very similar effects for a conventional violin geometry, since the underlying physical principles involved are the same.

2 FEA MODEL

For computational simplicity, we treat the violin as a shell structure with a smoothed guitar-shaped outline following the inner perimeter of the plates glued to the ribs, corner- and end- blocks of a del Gesu Guarnerius violin. For the purpose of these model calculations, the relatively small differences in the shapes and archings of different instruments and the small overhang of the plates over the ribs are unimportant. The rigid corner and end blocks are treated as rigid, increased mass sections of the ribs. The neck and fingerboard are also represented as shell elements, with physical dimensions, mass and elastic properties chosen to give typical measured bending and twisting

mode frequencies. We include a constant thickness bridge with a mass and cut-out waist to reproduce a planar rocking-mode resonance at ~ 2.5 kHz, proposed to explain the so-called BH peak in the radiated output observed for many violins[6]. The soundpost is modeled by a hollow cylinder with the same diameter and mass as a normal soundpost, with wall thickness and elastic constants chosen to reproduce the lowest flexural resonance of a solid post. Typical longitudinal and transverse arching profiles are modeled by 3rd-degree Bezier curves, with shapes and heights that can be varied independently. Because the COMSOL shell structure software does not yet support anisotropic materials, this is simulated by alternating strips of wood with low and high elastic constants give the same large-scale anisotropic elastic constants used by Roberts[4] in his analysis. We use a "grain spacing" of 1 cm, which is much less than the wavelength of all the flexural modes of immediate interest. However, for this approximation to be valid, the mesh size must be smaller than this dimension, which results in longer computation times.

For each eigen mode, we evaluate the eigen frequency and spatial displacements over the surface of the instrument. For each mode, the effective mass at the top of the bridge is determined by the peak kinetic energy E_k and associated velocities at the bridge parallel and perpendicular to the front plate. The admittance in the two directions is then given by

$$A^{\parallel,\perp}(\omega) = \sum_k \frac{\left(v_k^{\parallel,\perp}\right)^2}{2E_k} \frac{j\omega}{\omega_k^2 - \omega^2 + j\omega\omega_k / Q_k},$$

for eigen-frequencies ω_k and quality factors Q_k, which can be evaluated using complex values for the elastic constants or taken from typical measurements. To a good approximation, below ~ 700 Hz - where the acoustic wavelength is larger than the size of the instrument, one can use a multipole expansion to describe the intensity of the radiated sound as a function of frequency, with the strength of the dominant monopole and dipole sources evaluated by integrating the velocity distribution across all surfaces.

3 RIB COUPLING

To illustrate the overall philosophy of this investigation, we have used FEA to evaluate the frequencies of the normal modes and associated wave-functions (mode shapes) for a simplified guitar shaped shell with arched but isotropic plates before cutting the f-holes and inclusion of bass bar and soundpost. The instrument is freely supported, with light springs to restrain motion in the 6 degrees of freedom of the whole body about its centre of mass.

The guitar outline follows the geometric shape and arching of a Guarnerius del Gesu violin with 1.5 thick, 3cm high ribs. The top plate is 2.5 mm thick, with density 450 kgm-3 and isotropic elastic constant 7e9 Pa; the back plate is 3.5mm back plate with density 600 kgm-3 and isotropic elastic constant 1e10 Pa. To investigate the physics of the coupling of the front and back plates of the violin by the ribs, we varied the elastic constant of the ribs by many orders of magnitude. In Fig.1 we have plotted the predicted modal frequencies as a function of its elastic constant or coupling strength. The plate elasticity is varied from a very small value to that of the back plate.
We have also identified the modal shapes of the various branches of the modal diagram, with the ribs made transparent, to enable the modes of both plates to be viewed together.

For small rib coupling, the lowest frequency modes are flexural waves in the ribs themselves, which can exist - like waves in a waveguide - above a critical frequency

$$\omega_c \sim \sqrt{\frac{E}{12(1-\nu^2)\rho}}\, t\left(\frac{\pi}{h}\right)^2$$

where *t* and *h* are the rib thickness and height. This results in the band of rib modes with a different number of half-wavelength around the perimeter. The frequency of such modes varies as $E^{1/2}$, as illustrated by the logarithmic plot. There would be similar bands with 2, 3, 4, etc. half–wavelength across the ribs, and higher bands still for the equivalent longitudinal modes. Resonances of all

such modes can be ignored for all practical purposes. The ribs can therefore be considered as simple cantilever springs that tie the outer edges of the two plates together, which also inhibit bending at the edges of the plates.

The tying together of the plate modes at their perimeters results in a new set of initially hinged-plate modes, with flexural mode shapes illustrated on the right-hand side of Fig.1. Although the perimeters are closely ties together, they are not in general nodes, as the vibrations in the asymmetric shaped plates involve both linear and angular momentum about the centre of mass of the structure. To conserve the linear and angular momentum of a freely supported instrument, *the whole body* therefore has to translate and rotate in the opposite directions.

The lowest of these modes is the main shell breathing mode, with the two plates vibrating in opposite directions to give a net change of volume. This mode involves very little translation of the ribs as, to a first approximation, the linear momentum of the front and back plates are equal and opposite (Cremer[7]). This also explains why the amplitude of vibration of the lighter front plate is generally larger than that of the heavier back plate. In contrast, the higher frequency mode with both plates moving in the same direction requires a large amount of linear and rotational energy of the whole instrument to conserve linear and angular momentum.

As the coupling strength is increased the ribs become more resistant to bending, so the boundary condition around the perimeter of the plates changes from being hinged to fixed (no bending at their edges). This forces the wave vibrations to move away from the edges, increasing their elastic energy and hence frequency though not their ordering, as illustrated.

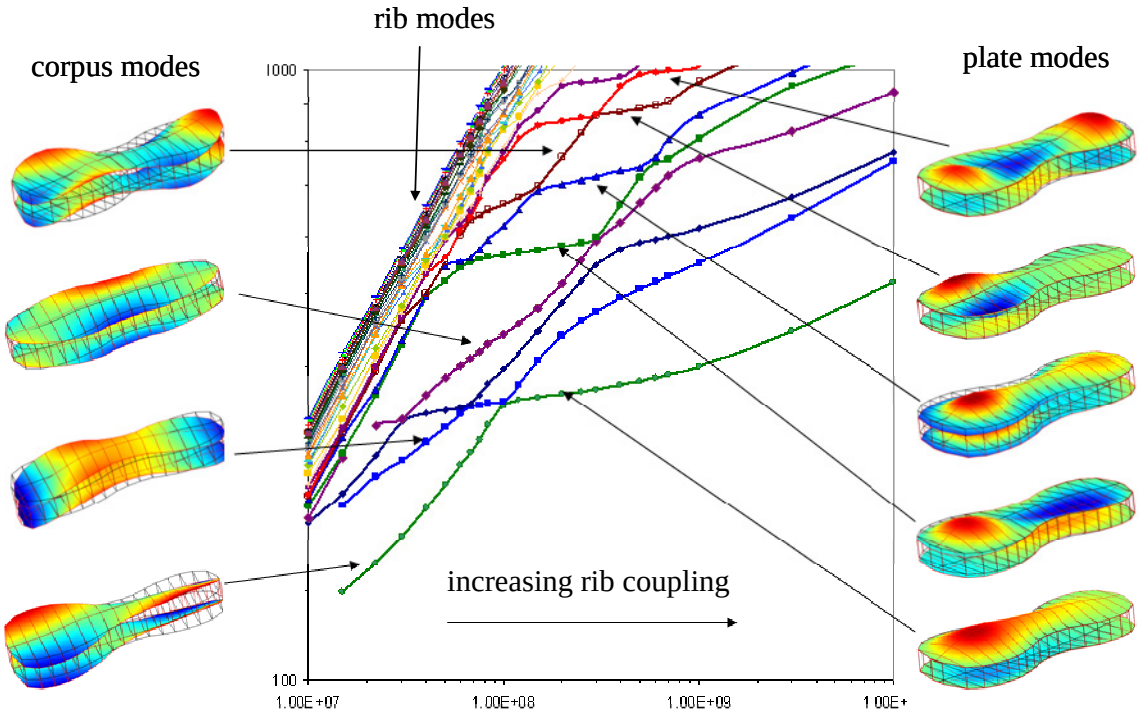

Figure 1 Modal frequencies and shapes as a function of the elastic properties of the ribs varying over several orders of magnitude.

Crossing the plate modes are an additional set of *corpus* modes illustrated to the LHS of Fig.1 involving the twisting, bending and flexing of the instrument as a whole with identical displacements of the top and back plates. They can be clearly distinguished from the *plate* modes by their very different dependence on rib coupling strength. Because the corpus modes involve no net changes in volume, they only contribute to the admittance at the bridge, but not to the radiated sound. In this

simplified model, the only modes contributing significantly to the radiated sound at low frequencies would be the lowest plate mode with a strong monopole moment and the higher plate modes with varying monopole and dipole components depending on the mode symmetry.

For a symmetric shell structure, the normal modes of different symmetries (symmetric or asymmetric) are uncoupled and their frequency branches simply cross without any perturbation (e.g. the lowest corpus and plate modes). However, corpus and plate modes sharing the same symmetry can be coupled leading to a perturbation and splitting of the modal branches as can be seen for a number of modes in Fig. 1.

Interestingly, in the present model, there is a negligibly small interaction between the longitudinal bending corpus mode and lowest plate breathing mode. In contrast, a natural explanation for nodal lines observed for the B1- and B1+ modes would imply a pair of normal modes formed from the in- and out-of-phase vibrations of the longitudinal bending mode and the strong flexural breathing mode. The addition of the neck, fingerboard and f-holes and the inclusion of anisotropy would be expected to perturb the modal frequencies somewhat, but would be unlikely to change the overall global features significantly. This simply leaves the soundpost as the main perturbing feature that could give rise to the double B1- and B1+ "breathing" modes, if they are to be interpreted in the way suggested.

4 INFLUENCE OF SOUNDPOST

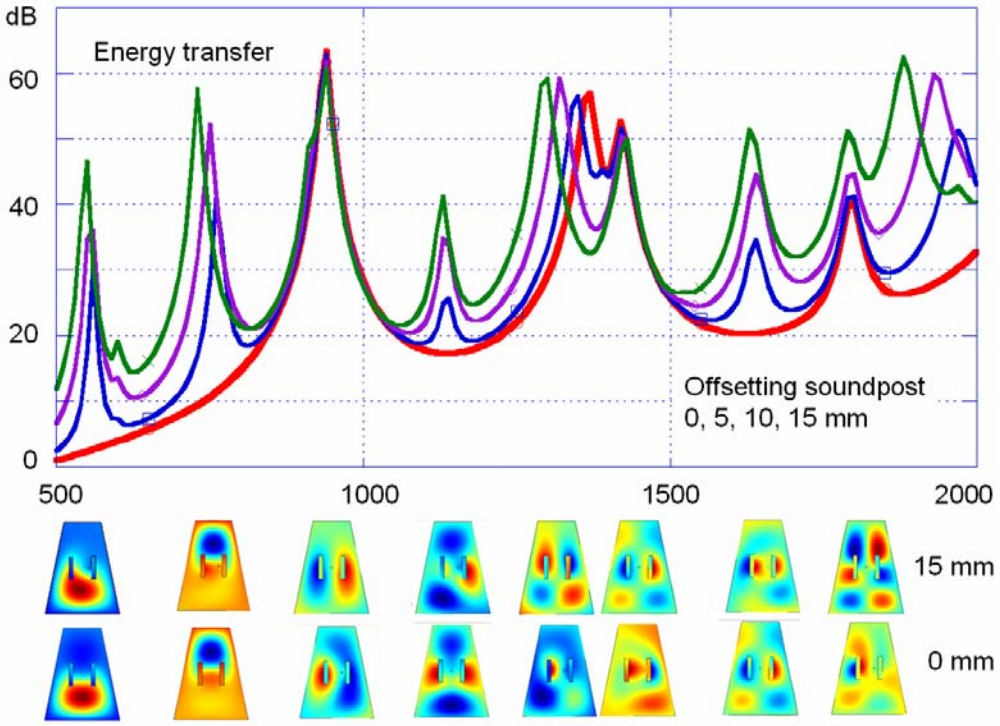

Figure 2 Changes energy transfer from rocking bridge to plate modes of a trapezoidal Savart violin and associated changes in mode shapes, as a function of offsetting sound post position from central position in steps of 5mm (red central soundpost to green 15mm offset)

In a preliminary investigation[5], we investigated the vibrational modes of a Savart trapezoidal violin as a function of soundpost position. A very simple model was used with rigid ribs and an isotropic flat trapezoidal plate with vertical slots with a rigid soundpost creating a node at its point of contact

with the top plate. In this study, the structure was driven by equal and opposite harmonic forces acting at the two bridge feet. The energy transferred to the structure was then determined as a function of driving frequency from the product of the forces and induced velocities at the two feet. . The plots in Fig.2 show the calculated energy transfer as the soundpost is offset from the central axis by 0, 5, 10 and 15mm.

The sound post and to a lesser extent the slots result in a significant reduction in the amplitude of the wave-function in the island area and a splitting of the lowest breathing mode into two higher frequency modes localized in the lower- and upper-bouts. The upper-bout mode is higher in frequency, because it is more constrained in size and hence the larger stored elastic energy. For a central soundpost, the couple exerted by the bridge can only excite weakly radiating asymmetric modes. The lower frequency symmetric modes would therefore make no contribution to the radiated sound. However, on progressively offsetting the soundpost, the symmetric modes are increasingly strongly excited, as illustrated. This would lead to a dramatic increase in radiated sound of around 10 dB to over 30 dB in the range 500-700 Hz, with very significant increases from symmetrical modes at higher frequencies as well, as shown.

Although soundpost position has such a strong effect on the radiated sound, it has a much smaller effect on modal frequencies. This is because the modal frequencies are largely determined by the wave amplitudes on the major surface areas of the lower and upper bouts rather than in the island area near the two bridge feet, where the perturbation of the soundpost is largest.

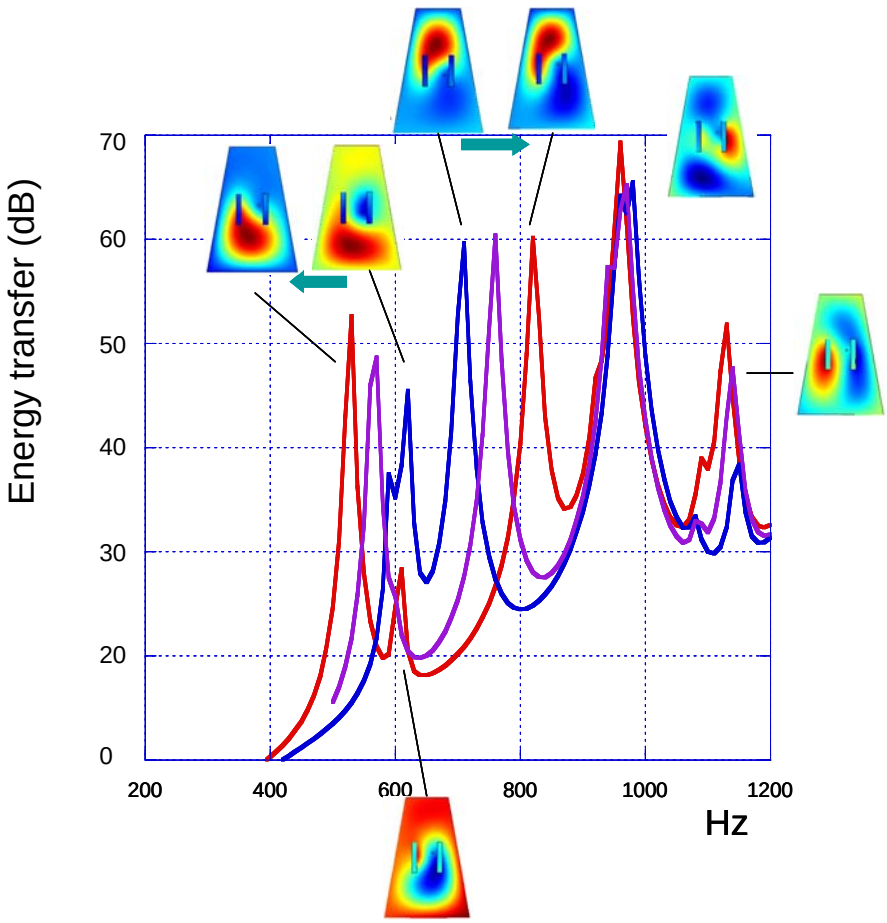

Figure 3. Effect on mode couplings, frequencies and mode shapes on moving soundpost 10 mm towards (red curve) and away (blue curve) from the upper bout from its 15mm offset position.

In Fig.3 we illustrate the effect of moving the 15mm offset sound post +10 mm and -10 mm towards and away from the upper bout. On moving the soundpost towards the lower bout, the lower bout breathing mode is “compressed” raising its frequency, while the upper bout breathing mode expands and lowers in frequency. This leads to a reduced separation in frequency of the modes. Moving the soundpost towards the upper bout has the opposite affect increasing the spacing between the modes and, in this case, significantly reducing the coupling to the lower mode as well.

One might expect to find rather similar effects for the violin, with changes in the position of the sound post making relatively little difference to modal frequencies but having a much larger affect on their coupling to the bowed string vibrations and hence radiated sound. Violin makers are sensibly rather conservative in shifting the soundpost by relatively small distances to optimize the quality of an instrument. Nevertheless, it would be interesting to investigate the differences in tone colour on making much larger changes in position

5 SUMMARY

These preliminary investigations provide valuable insight into the kind of calculations and problems to address using more realistic violin geometries. Even the simple models investigated reveal a number of interesting features that are probably generic to any shell model of the violin. In particular one can identify the CBR as a twisting mode of the central bout relative to the much stiffer upper and lower bouts. This also involves a shearing motion of the ribs relative to each other, as observed in the recent 3D-Strad project. Moreover, our model would suggest that it is the plate breathing modes rather than corpus bending modes that will be largely responsible for the radiated sound. It is therefore somewhat confusing that the strongly radiating B1- and B1+ modes should be described as bending modes. Further studies should clarify the relationship between these modes and the modes predicted by FEA. The strong dependence of mode frequencies and coupling to the vibrating strings indicated by our FEA analysis of the Savart Trapezoidal violin, suggest equally strong effects will also observed for a conventional violin.

6 REFERENCES

1 G. Bissinger. A unified materials-normal mode approach to violin acoustics, Acustica 91, 214-228 (2005)

2 G. Bissinger. Structural acoustics of good and bad violins (to be published)

3 G.A. Knott, *A modal analysis of the Violin, MSc Thesis 1987* (*Naval Postgraduate School, Monterey)* reproduced in *Research Papers in Violin Acoustics 1975-93.* Ed. C. Hutchins (Acoust. Soc. Am., 1996)

4 G.W. Roberts (1986) Finite Element Analysis of the Violin (PhD Thesis, Cardiff) reprinted in *Research Papers in Violin Acoustics 1975-1993*, Ed. C.Hutchins (Acoust.Soc. Am.)

5 C.E. Gough, The Violin: Chladni patterns, plates, shells and sounds inn *Nodal Patterns in Physics and Mathematics,* Eur. Phys. Jnl. – Special Topics 145, 77-102 (2007**)**

6. F.Durup and E. Jansson, The quest for the violin bridge-hill, Acustica 91, 206-213 (2005)

7 L. Cremer, *The Physics of the Violin* (MIT Press, 1984), Section 10.4